

Luttinger liquid ARPES spectra from samples of $\text{Li}_{0.9}\text{Mo}_6\text{O}_{17}$ grown by the temperature gradient flux technique

G.-H. Gweon^{†,1}, S.-K. Mo,¹ J. W. Allen,¹ J. He,² R. Jin,³ D. Mandrus,^{2,3} and H. Höchst⁴

¹*Randall Laboratory of Physics, University of Michigan, 500 E. University, Ann Arbor, MI 48109*

²*Department of Physics and Astronomy, University of Tennessee, Knoxville, TN 37996*

³*Solid State Division, Oak Ridge National Laboratory, Oak Ridge, TN 37831*

⁴*Synchrotron Radiation Center, University of Wisconsin, Stoughton, WI 53589*

(Dated: October 5, 2018)

Angle resolved photoemission spectroscopy line shapes measured for quasi-one-dimensional $\text{Li}_{0.9}\text{Mo}_6\text{O}_{17}$ samples grown by a temperature gradient flux technique are found to show Luttinger liquid behavior, consistent with all previous data by us and other workers obtained from samples grown by the electrolyte reduction technique. This result eliminates the sample growth method as a possible origin of considerable differences in photoemission data reported in previous studies of $\text{Li}_{0.9}\text{Mo}_6\text{O}_{17}$.

PACS numbers: 71.10.Pm, 71.20.-b, 79.60.-i

$\text{Li}_{0.9}\text{Mo}_6\text{O}_{17}$, also known as the Li purple bronze, is a quasi-one-dimensional metal which displays metallic T-linear resistivity and temperature independent magnetic susceptibility for temperatures down to $T_X \approx 24$ K, where a phase transition of unknown origin is signaled by a very weak anomaly in the specific heat¹. As T decreases below T_X , the resistivity increases. However the d.c. magnetic susceptibility is unchanged below T_X ^{1,2}, implying no single particle gap opening, and infrared optical studies³ below T_X also show no gap opening down to 1 meV. Consistent with this evidence for the lack of a single particle gap, repeated x-ray diffraction studies⁴ show no charge density wave or spin density wave.

The various transport and spectroscopy studies of this fascinating material have been made on samples prepared by two methods, an electrolyte reduction technique¹ and a temperature gradient flux technique⁵. Angle resolved photoemission spectroscopy (ARPES) is the only measurement for which any major inconsistency in data obtained from samples prepared by the two different methods has been reported, and the inconsistency is very serious. In particular an extensive set of ARPES data from two groups^{6,7,8,9,10,11,12} obtained on electrolyte reduction samples show non-Fermi liquid ARPES line shapes consistent^{7,9,10,11,12} with Luttinger liquid (LL) behavior and no low temperature Fermi energy (E_F) gap, whereas ARPES data reported^{13,14,15} for temperature-gradient-flux grown samples show Fermi liquid (FL) line shapes, a large low temperature E_F gap and an additional feature inconsistent with the known band structure of the material. These differences between the two ARPES data sets are summarized in Ref. [8]. The LL line shapes have been verified repeatedly in subsequent studies^{8,9,10,11,12} of samples prepared with the electrolyte reduction technique. Nonetheless it has been a lingering possibility that FL line shapes and a large low temperature gap could perhaps be characteristic of temperature gradient flux grown samples. This Brief Report dispels that possibility by reporting ARPES spectra for temperature gradient flux grown samples that are in full agreement with the

line shapes obtained for electrolyte reduction samples.

The spectra reported here were obtained on the PGM beamline at the Wisconsin Synchrotron Radiation Center. Photons of energy 30 eV were used to excite photoelectrons whose kinetic energies and angles were analyzed with a Scienta SES 200 analyzer. Measurement on a freshly prepared Au surface was used to determine the position of E_F in the spectra and the overall energy resolution of 21 meV due to both the monochromator and the analyzer. The angle resolution was set at $\pm 0.1^\circ$, better than that $\pm 0.25^\circ$ in our earlier work⁸ and exactly the same as used in previous ARPES studies^{13,14,15} of temperature gradient flux samples. The sample surface was obtained by cleaving *in situ* and the data were taken at a sample temperature of 200 K, much higher than the transition temperature 24 K.

For the endstation in place at the time of taking the data reported here, the angular dispersion direction of the SES 200 analyzer was vertical. ARPES symmetry analysis of the data obtained shows that the one dimensional Γ -Y chain axis direction was (unintentionally) oriented at an angle of 13° to the vertical. Nonetheless we will refer to this geometry as the “vertical geometry” from here on in the paper. Due to this small angular offset, the dispersions in this data set are slightly different from those that we obtained previously along the Γ -Y axis, as documented carefully in discussing Fig. 2 below. We have repeated the measurement in exactly the same geometry as that of our previous experiments^{7,8,9,10,11,12}, i.e. one in which both the one dimensional chain axis and the angular dispersion direction of the analyzer are horizontal and well aligned, and found dispersions essentially identical to those of the previous^{7,8,9,10,11,12} data. We will refer to this geometry as the “horizontal geometry” below. Despite the small angular offset, we present here the data taken in the vertical geometry because (1) these data happen to show the E_F -crossing line shapes most clearly among all of our data sets, by virtue of having fortuitously the maximum intensity of the band crossing E_F relative to the intensities of the bands that do

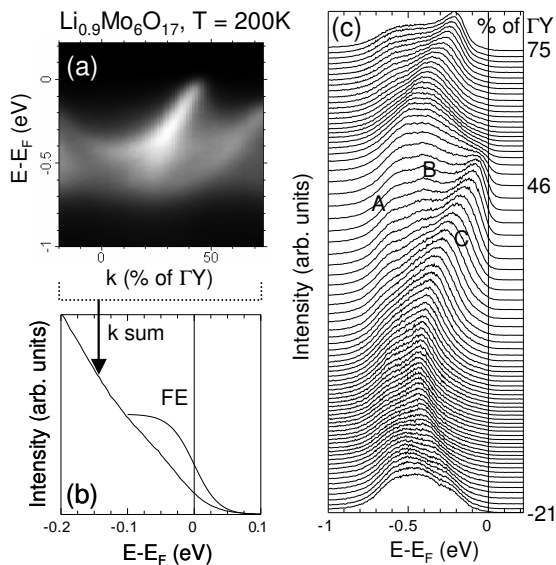


FIG. 1: ARPES data obtained for samples of $\text{Li}_{0.9}\text{Mo}_6\text{O}_{17}$ prepared by the temperature gradient flux growth. (a) k -energy map where k is the momentum projected onto the Γ - Y axis. (b) The k -sum of the data in (a). A Fermi edge (FE) spectrum for the employed energy resolution (21 meV FWHM) and the measurement temperature (200K) is shown to demonstrate the non-FE nature of the k -sum. (c) An energy distribution curve (EDC) stack representation of the data shown in (a). The spectrum corresponding to k_F is drawn with a thick line. The momentum increment is 1.3% of Γ - Y .

not cross E_F , and (2) the differences in dispersions have been verified to arise from the small offset and are in any case so slight as to be insignificant for the central thrust of this paper. Both of these points are elaborated below. Another advantage of the vertical geometry setup was that it allowed acquisition of intensity maps like the one presented below (Fig. 1) for many parallel one dimensional paths crossing the FS. Thereby we could verify that the LL behavior holds for such paths anywhere in the Brillouin zone, regardless of the exact location of the momentum space cut across the Fermi surface, so that Fermi liquid behavior does not occur for some very specific cut, as reported previously^{13,14} for temperature gradient flux samples.

Fig. 1 shows ARPES spectra taken in the vertical geometry on a sample grown by the temperature gradient method. Panels (a) and (c) summarize the overall electronic structure with k labels denoting the k values projected onto the Γ - Y axis. We label the bands A,B,C in the order of decreasing binding energy at Γ . As we will discuss in connection with Fig. 2 below, the overall band structure revealed by the data is consistent with the data in the literature^{6,7,8,9,10,11,12} obtained on samples grown by the electrolyte reduction method, as well as with band theory¹⁶. Furthermore, the LL line shapes observed previously^{7,8,9,10,11,12} are not just confirmed, but actually better observed due to the enhanced strength

of band C relative to that of bands A,B in the present data. For example, we can now clearly observe that the spectral weight of band C shows a back-bending behavior after the peak has crossed the Fermi level (darker curve), one of the key signatures of the LL line shape. In panel (b) we show the k -sum of the ARPES data. As found previously, the resulting line shape is far from the Fermi edge line shape expected of a FL and instead is described much better by a LL with $\alpha > 0.5$, where α is the so-called the anomalous dimension of the LL.

Panel (a) of Fig. 2 summarizes the overall band structure determined from the present data (open circles) and compares it with that from our previous result (diamonds) taken on a sample grown by the electrolyte reduction technique. The small differences arising from the slightly different k -paths can be seen. For example, in the new data band B becomes almost non-dispersive when peak C crosses E_F while this occurs for larger k values for the data perfectly along Γ - Y . As shown in panel (b) band theory predicts bands A, B, and C essentially as observed, and also a fourth band D. Bands A and B do not cross E_F and C and D become degenerate and cross E_F together. All four bands have been observed^{7,8,9} for various k -paths, although band D is typically very weak, just a slight shoulder on the leading edge of peak C, and is clearly seen only for a particular k -path^{7,10} where it appears as a main peak. In the vertical geometry data, band D is nearly undetectable (see Fig. 1 (c)) but was observed very weakly in the horizontal geometry data, consistent with previous results. For completeness, we mark the approximate position of band D thus found for the present sample as a gray region. This position is similar to that found for previous samples along the same, i.e. the Γ - Y , direction as well as along the special k -path^{7,10} where D is strong.

Fig. 3 compares the E_F crossing line shapes measured on the samples grown by the two different methods, with panel (a) showing the new data in the vertical geometry for the temperature gradient flux sample, and panel (b) showing data from Ref. [10] taken at the same photon energy for the electrolyte reduction sample. In each panel, the data are presented with the spectra for the various k -values overplotted to better show the approach and E_F crossing of peak C. As explained in the previous paragraph, a small difference of the band B dispersion arises from the slightly different k -paths. The general features of the two sets of spectra are nearly identical, except that, as mentioned already, in (a) the strength of band C relative to that of the non- E_F crossing band B is greater than in (b). Therefore the intrinsic line shape features of band C, which we have shown^{7,9,10,11,12} to be well described by the LL line shape theory, are now even more clearly visible. These include the spinon edge and the holon peak, which disperse with different velocities, the diminution of intensity as E_F is approached, and the back dispersing edge after the peak has crossed E_F . One is now forced to conclude that the large disagreement of the overall band dispersions and E_F crossing line

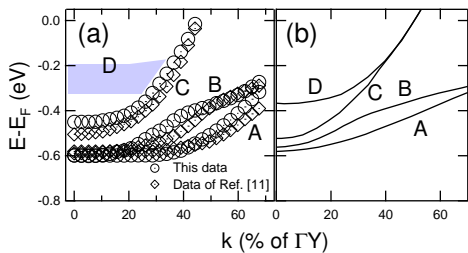


FIG. 2: Agreement of the overall band structures obtained on the two samples grown with different methods. (a) Momentum-energy dispersion relations as extracted by taking the peak positions of energy distribution curves (e.g. in Fig. 1 (c)). The data plotted in circles correspond to the data of the current sample (Fig. 1) grown by the temperature gradient flux method and the data plotted in diamonds correspond to the data reported in Ref. [10] for sample grown by the electrolyte reduction method. See text for discussion of small differences visible, arising from slightly different k -paths. The approximate position of the band D for both samples is indicated as a gray region. (b) Extended Hückel tight binding band structure calculation¹⁶ for comparison. Note that the energy scale of the calculation was multiplied by a factor of 2.2 in order to roughly match the dispersion of the experiment.

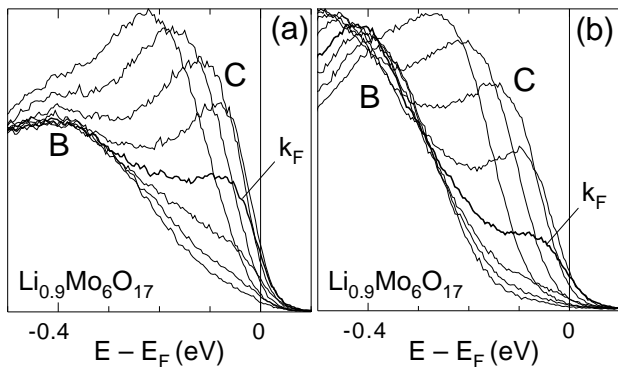


FIG. 3: Identical nature of LL ARPES lineshapes obtained for samples of $\text{Li}_{0.9}\text{Mo}_6\text{O}_{17}$ prepared by (a) the temperature gradient flux growth and (b) electrolyte reduction methods. The data in (b) is from Ref. [10]. In both panels, the momentum increment is 2.6% of Γ -Y.

shapes found previously⁸ for the ARPES data reported by Xue et al.^{13,15} and those reported by ourselves and others^{6,7,8,9,10,11,12} do not stem from the sample growth method.

Before concluding, we note that samples prepared by us [JH, RJ and DM] in the same way as for those used in the ARPES reported here, have also been used for new measurements of the temperature dependences of the resistivity, specific heat, magnetic susceptibility and optical properties¹⁷. These results have re-confirmed that no gap opening is associated with the low T resistivity rise and have been interpreted as showing the probable importance of localization effects for the properties below T_X . Although the lower energy limit of the new optical study is 10 meV, larger than the minimum energy of 1 meV of a previous optical study³, it is nonetheless smaller than the energy resolutions used in any ARPES studies on the material to date (≥ 15 meV). Further, the new optical study found that the spectral weight *increases* below T_X in the low energy sector (< 100 meV) for which previous ARPES studies^{13,14,15} on temperature gradient flux samples found a large gap opening ($2\Delta \approx 80$ meV).

To summarize, we have shown that the ARPES spectra of $\text{Li}_{0.9}\text{Mo}_6\text{O}_{17}$ samples prepared by temperature gradient flux growth display LL behavior the same as seen for samples prepared by the electrolyte reduction method, thus augmenting further the strong case for LL ARPES lineshapes already established by our past ARPES work on this material.

Acknowledgments

This work was supported by the U.S. NSF grant DMR-99-71611 and the U.S. DoE contract DE-FG02-90ER45416 at U. Mich. The ORNL is managed by UT-Battelle, LLC, for the U.S. DoE under contract DE-AC05-00OR22725. Work at UT was supported by the NSF Grant DMR 00-72998. The SRC is supported by the NSF Grant DMR-0084402.

[†] Current address: MS 2-200, Lawrence Berkeley National Laboratory, 1 Cyclotron Road, Berkeley, CA, 94720; Electronic address: gweon@umich.edu.

¹ C. Schlenker, H. Schwenk, C. Escribe-Filippini, and J. Marcus, *Physica* **135B**, 511 (1985).
² Y. Matsuda, M. Sato, M. Onoda, and K. Nakao, *J. Phys. C* **19**, 6039 (1986).
³ L. Degiorgi, P. Wachter, M. Greenblatt, W. H. McCarroll, K. V. Ramanujachary, J. Marcus and C. Schlenker, *Phys. Rev. B* **38**, 5821 (1988).
⁴ J. P. Pouget, private communication.
⁵ M. Greenblatt, W. H. McCarroll, R. Neifeld, M. Croft and J. V. Waszczak, *Solid State Comm.* **51**, 671 (1984).
⁶ M. Grioni, H. Berger, M. Garnier, F. Bommeli, L. Degiorgi and C. Schlenker, *Phys. Scripta* **T66**, 172 (1996).

⁷ J. D. Denlinger, G.-H. Gweon, J. W. Allen, C. G. Olson, J. Marcus, C. Schlenker and L. S. Hsu, *Phys. Rev. Lett.* **82**, 2540 (1999).
⁸ G.-H. Gweon, J. D. Denlinger, J. W. Allen, C. G. Olson, H. Höchst, J. Marcus, and C. Schlenker, *Phys. Rev. Lett.* **85**, 3985 (2000).
⁹ G.-H. Gweon, J. D. Denlinger, J. W. Allen, R. Claessen, C. G. Olson, H. Höchst, J. Marcus, C. Schlenker and L. F. Schneemeyer, *J. Elec. Spectro. Rel. Phenom.* **117-118**, 481 (2001).
¹⁰ G.-H. Gweon, J. D. Denlinger, C. G. Olson, H. Höchst, J. Marcus and C. Schlenker, *Physica B* **312-313**, 584 (2002).

- ¹¹ J. W. Allen, Solid State Commun. **123**, 469 (2002).
- ¹² G.-H. Gweon, J. W. Allen, and J. D. Denlinger, Phys. Rev. B **68**, 195117 (2003).
- ¹³ J. Xue, L.-C. Duda, K. E. Smith, A. V. Fedorov, P. D. Johnson, S. L. Hulbert, W. McCarroll, and M. Greenblatt, Phys. Rev. Lett. **83**, 1235 (1999).
- ¹⁴ K. E. Smith, J. Xue, L.-C. Duda, A. V. Fedorov, P. D. Johnson, W. McCarroll, and M. Greenblatt, Phys. Rev. Lett. **85**, 3986 (2000).
- ¹⁵ K. E. Smith, J. Xue, L.-C. Duda, A. V. Fedorov, P. D. Johnson, S. L. Hulbert, W. McCarroll and M. Greenblatt, J. Elec. Spectro. Rel. Phenom. **117-118**, 517 (2001).
- ¹⁶ M.-H. Whangbo and E. Canadell, J. Am. Chem. Soc. **110**, 358 (1988).
- ¹⁷ J. Choi, J. L. Musfeldt, J. He, R. Jin, J. R. Thompson and D. Mandrus, Phys. Rev. B, **69**, 085120 (2004).